Injury, Int. J. Care Injured 50 (2019) 834–847

Contents lists available at ScienceDirect

Injury

journal homepage: www.elsevier.com/locate/injury

Heterologous fibrin sealant potentiates axonal regeneration after peripheral nerve injury with reduction in the number of suture points

Ana Paula Silveira Leite[a,b,*], Carina Guidi Pinto[a,b], Felipe Cantore Tibúrcio[b], Arthur Alves Sartori[b], Antonio de Castro Rodrigues[d], Benedito Barraviera[c], Rui Seabra Ferreira Junior[c], André Luis Filadelpho[b], Selma Maria Michelin Matheus[b]

[a] Graduate Program on the General Bases of Surgery, Botucatu Medical School, Department of Anatomy, Universidade Estadual Paulista "Júlio de Mesquita Filho", São Paulo State University (Unesp), Institute of Biosciences, Travessa da Rua Prof. Dr. Gilberti Moreno São Paulo, 18618-689, Botucatu, Brazil
[b] Department of Anatomy, Universidade Estadual Paulista "Júlio de Mesquita Filho", São Paulo State University (Unesp), Institute of Biosciences, Travessa da Rua Prof. Dr. Gilberti Moreno São Paulo, 18618-689, Botucatu, Brazil
[c] The Center for the Study of Venoms and Venomous Animals, UNESP, Botucatu, SP, Brazil
[d] Unifai-Centro Universitário de Adamantina, Adamantina, SP, Brazil

ARTICLE INFO

Keywords:
Peripheral nerve injury
Neuromuscular interaction
Suture and heterologous fibrin sealant

ABSTRACT

The use of suture associated with heterologous fibrin sealant has been highlighted for reconstruction after peripheral nerve injury, having the advantage of being safe for clinical use. In this study we compared the use of this sealant associated with reduced number of stitches with conventional suture after ischiatic nerve injury. 36 Wistar rats were divided into 4 groups: Control (C), Denervated (D), ischiatic nerve neurotmesis (6 mm gap); Suture (S), epineural anastomosis after 7 days from neurotmesis, Suture + Fibrin Sealant (SFS), anastomosis with only one suture point associated with Fibrin Sealant. Catwalk, electromyography, ischiatic and tibial nerve, soleus muscle morphological and morphometric analyses were performed. The amplitude and latency values of the Suture and Suture + Fibrin Sealant groups were similar and indicative of nerve regeneration.The ischiatic nerve morphometric analysis in the Suture + Fibrin Sealant showed superior values related to axons and nerve fibers area and diameter when compared to Suture group. In the Suture and Suture + Fibrin Sealant groups, there was an increase in muscle weight and in fast fibers frequency, it was a decrease in the percentage of collagen compared to group Denervated and in the neuromuscular junctions, the synaptic boutons were reestablished.The results suggest a protective effect at the lesion site caused by the fibrin sealant use. The stitches reduction minimizes the trauma caused by the needle and it accelerates the surgical practice. So the heterologous fibrin sealant use in nerve reconstruction should be considered.

Introduction

In vertebrates, skeletal striated muscle requires innervation of the motor nerve to produce skeletal muscle contractions and to avoid muscular atrophy [1]. The region of contact between motor neurons and their target muscle fibers is a morphologically distinct region called the neuromuscular junction (NMJ), which is responsible for electric signal transmission from the motor neuron to the mucle fibers, promoting muscle contraction. In order for muscular contraction to occur, structures that promote neuromuscular interaction must be intact [2,3].

Several factors may determine changes in neuromuscular junctions, including peripheral nerve lesions (PNLs), which result in a loss of the connection between the axon and the muscle, leading to degeneration of these structures [4].

Peripheral nerve lesions constitute a common clinical scenario, and can lead to various complications and lifestyle impairments for the patients. These lesions affect approximately 13,9 individuals per 100 thousand, each year [5], and may lead to sensorial and or motor loss besides chronic pain [6,7].

When the injury occurs by complete transection of the nerve, with electrical conduction blockage, it is classified as neurotmese [8]. Following the injury, distally to the lesion causes a disconnection of the axons and their cellular bodies, leading to muscle denervation. Axonal regeneration, although limited, occurs

* Corresponding author at: Botucatu Medical School, Department of Anatomy, Institute of Biosciences (IBB), Universidade Estadual Paulista "Júlio de Mesquita Filho", Street Prof. Dr. Gilberti Moreno São Paulo, 18618-689, Botucatu, Brazil.
E-mail addresses: apsleitebio@hotmail.com, selma.matheus@unesp.br (A.P.S. Leite).

https://doi.org/10.1016/j.injury.2019.03.027
0020-1383/

spontaneously in the peripheral nervous system. Functionally, axonal regeneration is the replacement of the injured distal nerve segment, allowing for the reinnervation of the target organs and the reestablishment of their functions. Although there is a potential for spontaneous regeneration, functional recovery after nerve damage is limited in adults [9].

The gold standard for reconstruction in this type of lesion is end-to-end neurorrhaphy [10,11], although the use of sutures may lead to inflammatory reactions including the formation of granuloma and neuroma and leading to chronic pain [12,13]. An alternative to minimize the damage caused by suture use is to reduce the points used for reconstruction [14]. In this regard, the fibrin glue is a good strategy due to its adhesion capacity to tissues, and has been widely used in the medical field since the 70's [15]; however, there is an important disadvantage of the fibrin glue, since it contains human blood-derived fibrinogen, potentially leading to adverse reactions [12,13].

The Center for the Study of Venoms and Venomous Animals (CEVAP-Unesp-Botucatu-SP) has developed a fibrin adhesive derived from the venom of the snake *Crotalus durissus terrificus* and is considered a biological and biodegradable heterologous sealant that does not produce adverse reactions. Because it is free of human blood, it is not a transmitter of infectious diseases, as well as having a good adhesive capacity, and is indicated for use along with traditional suture procedures [16], in its composition, the cryoprecipitate containing fibrinogen and coagulation factors are derived from buffalo blood, and the functional thrombin is replaced by gyroxin, a thrombin-like protein also capable of cleaving fibrinogen in fibrin monomers [17]. This heterologous sealant have been tested with success in animals and human beings [18–20] in peripheral nerve lesions repair this sealant has shown promising results [21,22].

Even with advances in surgical procedures, nerve reconstructions result in only about 51% of motor recovery [23]. While many studies show that there is a morphological regeneration of the nerve and muscle, this is not associated with a functional recovery, and although there is axonal regeneration with normal morphology of Neuromuscular junctions, the failure of the muscular electrical activation is persistant [23]. Therefore, in addition to the nerve and muscle fibers, neuromuscular junctions should also be considered in these types of analyses, as well as the functional response resulting from these interactions. The fibrin sealant emerges as a potential, risk-free adjuvant to the regeneration process, when associated to the suture, allowing for reduction in the number of points and acting as a support, contributing to the axonal growth microenvironment [14].

Therefore, the objective of this study was to evaluate the use of heterologous fibrin sealant associated with a reduced number of stitches (1 point) when compared with conventional suture (3 stitches) after ischiatic nerve injury. The morphological and functional aspects of neuromuscular interaction were evaluated.

Materials and methods

The study was approved by the Animal Research Ethics Committee of the Botucatu Medical School, UNESP, Brazil, under protocol no.1172/2016. Thirty - six male adult Wistar rats (UNESP / Botucatu / SP / Brazil) weighing between 300–400 g, were divided into 4 experimental groups: 1- Control (C); 2- Denervated (D); 3- Suture (S); 4- Suture + Fibrin Sealant (SFS). Animals were kept in an environment with controlled temperature and light.

Surgical procedure

The rats were anesthetized by intraperitoneal injection of Ketamine (Dopalen - 90 mg / kg) and Xylazine (Rompun - 10 mg / kg) and the right ischiatic nerves were exposed. Nerve injury was performed by complete transection of the nerve using a standard method, about 3 mm distal to its place of origin in the Denervated (D), Suture (S) and Suture + Fibrin Sealant (SFS) groups. In the group Denervated, in order to avoid spontaneous regeneration, a 6 mm fragment of the sciatic nerve was removed. Upon neurotmesis, the proximal and distal stumps were inverted 180° and fixed in the adjacent musculature, and sutured with simple points such as the soft tissues. In the group Control, after localization of the sciatic nerve, the skin was sutured.

Seven days after neurotmesis, a new incision was made, and the nerve stumps were subjected to end-to-end neurorrhaphy. In the Suture group, three single points of Mononylon 7-0 were used and in the Suture + Fibrin Sealant group (SFS) one point of suture was used, in addition to 100 μL of Heterologous Fibrin Sealant (CEVAP/ Brazil), which has its components and application formula listed in the patents (Registration numbers: BR1020140114327 and BR1020140114360) [24]. Sixty days after nerve reconstruction, all animals were weighed and anesthetized by intraperitoneal injection of Ketamine (Dopalen 90 mg/Kg) and Xilazine (Rompun 10 mg/Kg) to perform eleneuromyography and then euthanized with tiophental sodim (50 mg/Kg). The right soleus muscle were dissected, weighed and their middle third were separeted, individually. The proximal and distal portions of the soleus muscle were frozen in liquid nitrogen and stored in a biofreezer, at −80 °C. The ischiatic nerve and muscle branch of the tibial nerve for the soleus muscle were also collected.

Electroneuromyography

This analysis was performed in groups Control, Suture and Suture + Fibrin Sealant; in group Denervated, the lack of integrity of the ischiatic nerve prevented study.

Electroneuromyography was performed at the end of the study. It were used three electrodes: active, reference and dispersive for the action potential values. The active electrode was inserted into the ischiatic nerve proximal to injury, the reference electrode in the cranial tibial muscle, and the dispersive was introduced into the trunk (distant from the test site). The electrodes recorded the amplitude and latency of the muscle action potential. These date were recorded simultaneously by the Shappire II 4ME/ UNIPEX/ Botucatu/SP/Brazil.

Gait analysis using the "Catwalk" system

This evaluation was performed before surgery, and on the 15th, 30th and 60th days after sectioning and nerve reconstruction in all animals according to the experimental groups. A Catwalk XT 9.1- Noldus system was used, where the animal crossed an illuminated glass platform, monitored by a video camera associated with a footprint analysis software. The functional index of the fibular nerve [25] was obtained using the following formula: PFI = 174.9 ((EPL-NPL) / NPL) + 80.3 x (ETS-NTS) / NTS) - 13.4, in which E refers to the injured side and N to the uninjured side, TS refers to the distance between the first and fifth fingers (toe spread) and PL to the distance between the third finger and the heel (print lenght). For the other parameters, the results were expressed as mean of the ratios of the injured / uninjured sides of the plantar impressions, in order to perform and analyze the gait of the animal more completely.

Morphological and morphometric analysis of the sciatic nerve and the tibial nerve muscle branch for the soleus muscle

After removal the nerves were fixed in Karnovsky and postfixed and stained with 1% osmium tetroxide. Cross sections of

approximately 2 μm were obtained and photomicrographs were taken (Olympus Bx41, SC30 camera). Five random fields were used for morphometric analysis of the sciatic nerve (5% of the sample); for the tibial nerve the whole sample was used. The number, diameter and area of the axons and the nerve fibers were obtained, and from these, the thickness of the myelin sheath and the G-ratio were calculated. For the calculation of the number of axons and nerve fibers of the sciatic nerve, we used a ratio witch considered the calculated sample in relation to the total nerve [26].

Analysis of muscle fibers and percentage of collagen (n = 5)

In the proximal portions of the frozen soleus muscle, microtomy (8 μm), was performed, and 4 slides were prepared for each animal in each experimental group: first-HE, second-Picrossirius Red and third and fourth immunohistochemistry for Fast and Slow fibers, respectively. Slides were photographed at 200X magnification (Olympus Bx41, SC30 camera). HE staining was used for overall morphological analysis and morphometry of the muscle fibers area (200 muscle fibers from 3 to 4 random fields). This analysis was performed using "Image J" software [27]. Slides stained with Picrossirius Red was used to quantify the percentage of collagen (Leica QWin software) where automatic detection of red were used to determine the percentage of collagen. The third and fourth sides were subjected to immunohistochemistry using specific primary antibodies (Anti-myosin fast/Novocastra/1:130 and Anti-myosin slow/Novocastra/1:180). Histofine® (Multi-Nichirei) was used as the secondary antibody. The specific staining was revealed by the chromogenic substrate DAB (1:50). The frequency of muscle fiber types was calculated using the "Image J" software [27].

Protein quantification (Western Blotting) of PCNA (cell proliferation) and PAX7 (satellite cells), n = 5

The distal portions of the soleus muscle were homogenized in RIPA and protease inhibitors (30 mg of tissue/100 μl of extraction buffer). Tissue extracts were obtained by centrifugation for 10 min at 14,000 rpm at 4 °C. Protein content was determined by the Bradford method (Bio-Rad protein assay) and 75 μg of protein was used for analysis in polyacrylamide gel. After electrophoresis, the material was transferred to nitrocellulose membranes followed by blocking with 3% skim milk in TBS-T for one hour and then incubated with the primary antibodies (PaX7 / ab199010 1: 200-PCNA / ab29 / 1 : 150). Following the wash step, the membranes were incubated for one hour in secondary antibody and revealed using a quimioluminescent substrate for Western blotting (AMERSHAM ECLTM PRIME, GE Healthcare). Semiquantitative analysis of band densitometry was performed by Image J. Software [27]. Data were normalized using GAPDH (Cell Signaling).

Morphological and morphometric analysis of Neuromuscular Junctions by light microscopy (nonspecific esterase), (n = 5)

The middle third of the right soleus muscles was fixed in Karnovsky's solution, sectioned longitudinally with razor blade and subjected to the Non-specific Esterase reaction [28], in order to characterize neuromuscular junctions. Slides were photographed (200 x)-(Olympus Bx41(camera SC30) and measurements were taken from the area of 50 neuromuscular junctions, which were analyzed using "Image J" [27].

Ultrastructural analysis of muscle fibers and neuromuscular junctions (NMJs), (n = 3)

The muscular thirds were reduced into rectangular fragments in order to obtain longitudinal sections of the associated fibers and neuromuscular junctions. This material was processed and photodocumented according to the routine of the Electronic Microscopy Center of the Institute of Biosciences (CME / IBB / UNESP) in an Electronic Transmission Microscope (TECNAI Spirit Fei Company).

Statistical analysis

The results were expressed as mean and standard deviation, and statistically significant differences were considered when $p < 0.05$. For the analysis of Amplitude and Latency, area and diameter of axons and nerve fibers, myelin sheath thickness, G ratio, soleus muscle weight, collagen percentage, protein quantification of Pax7 and PCNA and muscle fiber area and JNMs, analysis of variance for the model with one fator were applied complemented by Tukey's multiple comparison test [29]. For analysis of animal weight and time of contact, it was used analysis of variance for the model of repeated measurements in independent groups complemented by the multiple comparisons test of Bonferroni [30]. For the number of axons and nerv1e fibers, a non-parametric analysis of variance (Kruskal-Wallis) was used for the model with a factor complemented with by Dunn's multiple comparison test [29]. For the area of the footprint, the ratio of maximum contact area and the Fibular Functional Index, a nonparametric analysis of variance was used for the replicate measures model in independent groups complemented by Dunn's multiple comparison test [30].

Results

*Electroneuromyography**

Electroneuromyography analysis was performed in the animals of groups Control, Suture and Suture + Fibrin Sealant, through which amplitude and latency values were obtained. Regarding Amplitude, mean values were higher in group Control (23.04 ± 6.52) when compared with Suture (7.10 ± 4.56) and Suture + Fibrin Sealant (8.40 ± 5.46) (Fig. 1-A). The mean values of the Latency values were lower in group Control (1.39 ± 0.40), compared with the lesion groups: Suture (2.59 ± 0.74) and Suture + Fibrin Sealant (2.66 ± 1.51) (Fig. 1-B). The lesion groups did not show statistical differences when compared the electroneuromyography parameters analyzed.

Evaluation of animal gait using the "Catwalk"

Gait parameters, assessed before surgery, did not show differences in all animals from all experimental groups. On the 15th day, post surgery, there was a difference between the groups when we compared the ratios of the footprint areas, with the higher ratio found in group Control, followed by group Denervated. The lower values were detected in the groups Suture and Suture + Fibrin Sealant. On the 30th postoperative day, the footprint ratios followed the same pattern described on the 15th day for the experimental groups (Fig. 2-B).

The other parameters also showed differences on the 30th day. The ratio of contact time was lower in all experimental groups when compared with Control(Fig. 2-A). The highest values in relation to the ratio of the maximum contact area of the legs with the platform were observed in group Control, followed by group Denervated, with the lowest values shown by groups Suture and Suture + Fibrin Sealant (Fig. 2-C). Regarding the Functional Index of the Fibular, the highest values were those of the groups Control and Denervated, whereas the groups Suture and Suture + Fibrin Sealant had the lowest values (Fig. 2-D).

On the 60th postoperative day, the groups Denervated, Suture and Suture + FibrinSealant had lower values when compared with

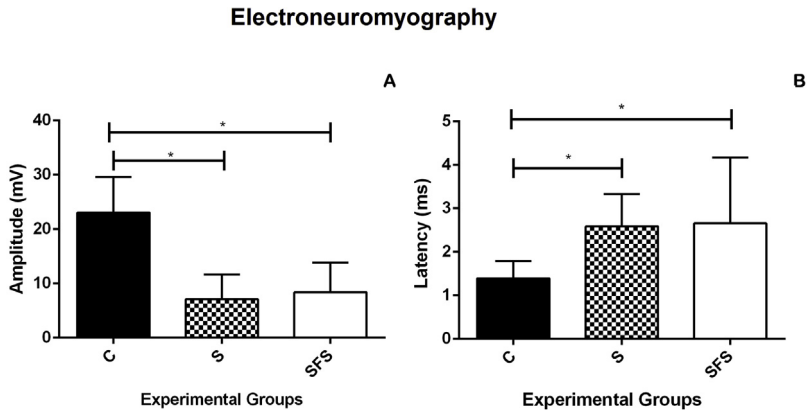

Fig. 1. Graph of the values obtained in Electroneuromyography showing Mean ± Standard Deviation (SD) of the Amplitude and Latency values in all experimental groups. A: amplitude values (mV); B: latency (ms); (Technique of analysis of variance for the model with one factor complemented by Tukey test of multiple comparisons (Zar, 2009), *$p < 0.05$).
*This analysis was not performed in the group D animals, due to the absence of integrity of the sciatic nerve.

group Control in relation to the areas of maximum contact and footprint and in the functional index of the Fibular nerve (PFI) (Fig. 2- B, C and D). The ratio of contact time was higher in group Control, followed by group Suture. Groups Denervated and Suture + Fibrin Sealant had the lowest values related to this parameter (Fig. 2-A).

Weight of the animals and of the soleus muscle

The final weight of the animals from all experimental groups was statistically significantly higher when compared to their initial weight. When the groups were compared, there was no difference between them at the beginning and at the end of the experiment. Regarding the weight of the soleus muscle, group Control animals had the higher values, followed by animals from the groups Suture and Suture + Fibrin Sealant. In these groups, the weight of the soleus muscle was statistically similar between them, and different from the other groups, showing lower values compared with group Control and higher values compared to group Denervated, which in turn had the lowest value (Fig. 3).

*Morphological and morphometric analysis of the ischiatic nerve and the tibial nerve muscle branch for the soleus muscle**

Histological images of both nerves in group Control showed an axon and integral myelin sheath, with morphology within the normality pattern (Fig. 4-A e 5-A). The tibial nerve general morphology was indicative of degeneration in group Denervated (Fig. 5-B). In the ischiatic nerve it was not possible to identify axons and nerve fibers. In Suture and Suture + Fibrin Sealant groups, in relation to both nerves, the morphology showed axons and nerve fibers remyelinated when compared with group Denervated, although the axons seemed to be smaller and irregular in relation to Control (Fig. 4-B and C and 5-C and D).

In the morphometric analysis of the ischiatic nerve, the values referring to the axon area, fiber area and axon diameter showed the

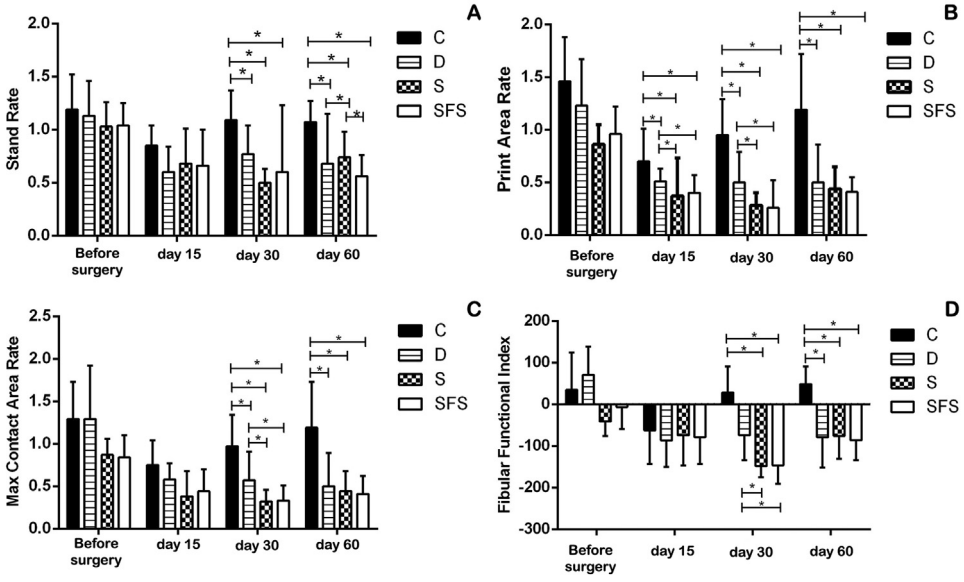

Fig. 2. Graphs of the means and standard deviation of the functional analyses (Catwalk) for the experimental groups at the different times. A: Ratio of contact time; B: Ratio of the footprint area (cm); C: Ratio of maximum contact area; D: Functional Fibular Index. The values in A, B, C are expressed as the ratio of the injured/uninjured sides of the plantar impressions. In A: Technique for analysis of variance for the model of repeated measurements in independent groups complemented by the Bonferroni multiple comparison test (Johnson & Wichern, 2007), * $p < 0.05$. In B, C and D: nonparametric analysis of variance for the repeated measures model in independent groups complemented by Dunn's multiple comparison test (Johnson & Wichern, 2007), *$p < 0.05$.

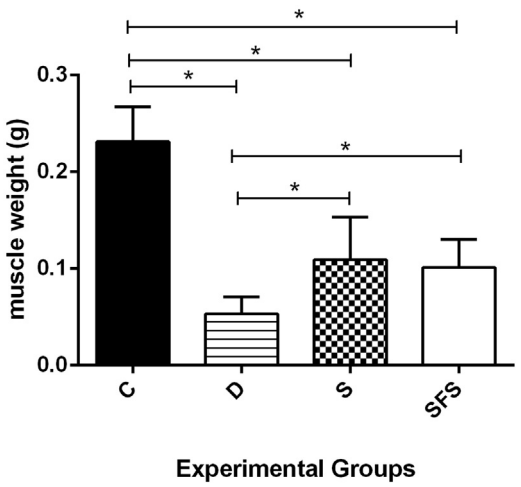

Fig. 3. Graph of the means and weight deviation (g) of soleus muscle in all experimental groups.(Technique of analysis of variance for the model with one factor complemented by test of multiple comparisons of Tukey (Zar, 2009), $^{*}p < 0.05$).

same statistical pattern, with the highest values presented by group Control, followed by the values of the Suture + Fibrin Sealant group, and with the group Suture having the lowest values among all groups (Fig. 4-D, E and G). Regarding the diameter of the nerve fibers, the groups Control and Suture + Fibrin Sealant showed similar results, followed by the lower values shown by group Suture (Fig. 4-H). Regarding the number of axons and fibers, the highest values were those of group Control, followed by the values of groups Suture and Suture + Fibrin Sealant, with no difference between them (Fig. 4-F). The results of myelin sheath thickness and G ratio were statistically similar in the 3 experimental groups (Fig. 4 I and J).

The morphometric analysis of the tibial nerve revealed a statistical pattern among the groups where the values for the number of nerve fibers and axons, area of nerve fibers and axons, minimum diameter of nerve fibers and axons and thickness of myelin sheath showed higher values in the animals of group Control when compared to the groups Suture and Suture + Fibrin Sealant (Fig. 5 E–J). The G ratio values were lower in group Control when compared with Suture and Suture + Fibrin Sealant groups (Fig. 5 K). On the other hand, the animals of the lesion group (Suture and Suture + Fibrin Sealant) were not statistically significantly different when the parameters described above were analyzed.

Analysis of muscle fibers and percentage of collagen

In group Control, the morphological analysis performed after HE staining showed characteristics compatible with normality: muscle fibers in polygonal format and with peripheral nuclei (Fig. 6A). Ultrastructurally, the myofibrils were well organized forming intact sarcomeres with morphological characteristics closely related to the different muscle types. A linear Z-line, intermiofibrillary mitochondria of variable sizes and T-tubules organized in triads were highlighted, as well as peripheral nuclei (Fig. 7A).

HE staining analysis showed, in group Denervated, agglomerates of small fibers, some of them with a rounded shape and others with a central nucleus (Fig. 6B). Ultrastructurally, in most myofibrils there was no organization in sarcomeres, with some regions containing only bundles of myofibrils, and a fragmented and scattered Z-line. Focal areas of lesion were present showing myelin figures and concentration of mitochondria; and central nuclei were abundant (Fig. 7B).

An intermediate morphology was observed in the Suture and Suture + Fibrin Sealant groups, with fibers with rounded shape and others with central nuclei visualized by HE staining (Figs. 6C and 6D). The ultrastructure revealed the recovery of muscle tissue where the sarcomeres were organized; focal areas of lesion were still present. The presence of papillary projections on the surface of the muscle fiber membrane was also observed in groups Denervated, Suture and Suture + Fibrin Sealant (Figs. 7C and 7D).

Regarding the fiber area, group Control animals showed the highest values. The animals in groups Denervated and Suture + Fibrin Sealant presented the lowest values, and those in group Suture had intermediate values (Fig. 6E).

Group Denervated presented the highest percentage of collagen, followed by groups Suture and Suture + Fibrin Sealant, while group Control had the lowest percentage values (Fig. 6F).

By the immunohistochemical staining, it was observed that the types of muscular fibers of group Control were organized in a mosaic. In groups Denervated, Suture and Suture + Fibrin Sealant there were areas with grouping of fiber types ("Type grouping") (Fig. 8-F). In relation to the frequency of Slow fiber types, group Control (183/155; 198) had the highest amount of this type of fibers, being statistically superior to the others; the animals of groups Denervated (143/125; 181) and Suture + Fibrin Sealant (153/85; 172) showed intermediate values, which were similar to each other and different from the other groups. The lowest values were those presented by group Suture (134/123; 163), which were still statistically inferior to the others (Fig. 8-D). The frequency of the Fast fibers was higher in the Suture + Fibrin Sealant group (76/40; 127), followed by the Denervated (58/57; 77) and Suture (75/49; 93) groups; while group Control had the lowest values (28/24; 55) (Fig. 8-E).

Protein quantification (Western Blotting) of PCNA (cell proliferation) and PAX7 (satellite cells)

Regarding quantification of PCNA and PAX7 proteins, there was no statistically significant difference between the experimental groups (Fig. 9).

Morphological and morphometric analysis of Neuromuscular Junctions

Using the non-specific esterase, was observed that the neuromuscular junctions were aligned to the largest axis of the muscle fibers, in all animals of the experimental groups.

In group Control, its distribution was restricted to the muscular middle third, with a highly branched, broad synaptic gutter with transverse striations corresponding to the junctional folds (Fig. 10-A). Ultrastructurally, several synaptic knobs were observed, arranged in synaptic gutter with varied shapes and depth. In the synaptic bottons, synaptic vesicles, mitochondria and multivesicular bodies were present. Characteristically, the presynaptic membrane had more electrondense regions that correspond to the active zones, opposite the apex of the junction folds of the postsynaptic membrane. The post-synaptic membrane was intact and contained numerous long junctions, with a more electrondense apex corresponding to the site of concentration of acetylcholine receptors (Fig. 11-A).

In group Denervated, the appearance was compact and broad, with the neuromuscular junctions sparsely distributed in relation to the middle third (Fig. 10-B). Degeneration of the pre-synaptic region was detected through the ultrastructure, leaving only junction folds, and it was not possible to distinguish the active zone (Fig. 11-B).

In the Suture and Suture + Fibrin Sealant groups the morphology was intermediate to the previous ones, with distribution of

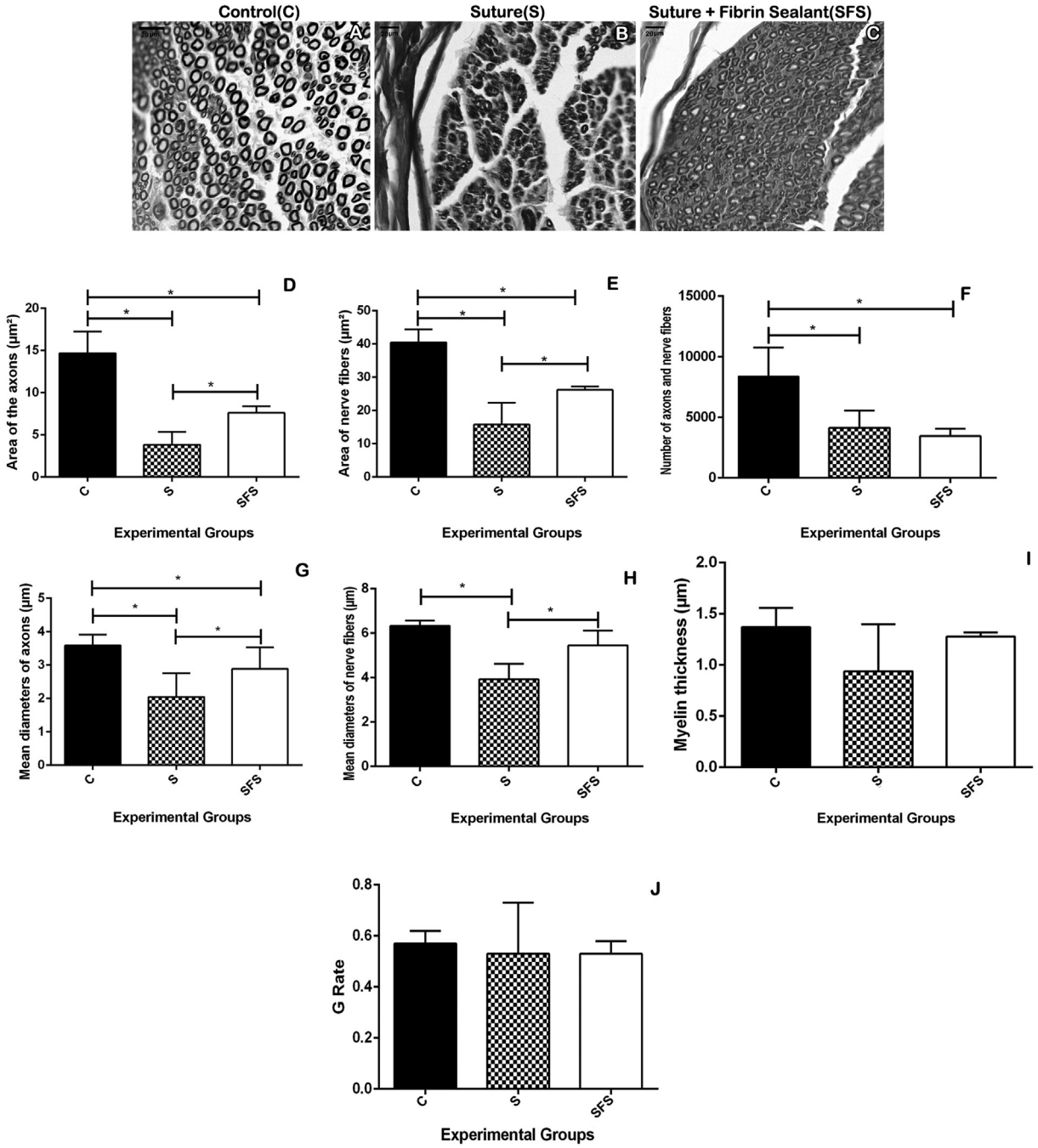

Fig. 4. A–C: Photomicrographs of transverse sections of ischiatic nerve, stained in osmium tetroxide. A: Control group (C); B: Suture group (S); C: Suture + Fibrin Sealant (SFS). D-J: Graphs showing the Mean and Standard Deviation values corresponding to the morphometric analysis of the sciatic nerve in the groups C,S and SFS. D: Area of axons (μm^2); E: Area of nerve fibers (μm^2); F: number of axons and nerve fibers. G: diameter of the axon (μm); H: diameter of nerve fibers (μm); I: Thickness of myelin sheath (μm); J: ratio G. D,E,G-J : Technique of analysis of variance for the model with one factor complemented by test of multiple comparisons of Tukey (Zar, 2009), *$p < 0.05$. F: Technique for analysis of non-parametric variance (Kruskal-Wallis test) for the model with factor complemented by Dunn's multiple comparison test (Zar, 2009),* $p < 0.05$).
*This analysis was not performed in group D animals, due to the absence of regenerated nerve fibers.

neuromuscular junctions in addition to the middle third (Fig. 10-C and D). Some synaptic gutter observed ultrastructurally were unoccupied, although some synaptic knobs presented variable morphology. Myelin figures, large numbers of synaptic vesicles and cellular debris were present. At the apex of the junction folds small regions of variable electron density were detected (acetylcholine receptors concentration) (Fig. 11-C and D).

The neuromuscular junction area presented lower values in group Denervated when compared with group Control ($p = 0.03$). The groups Suture and Suture + Fibrin Sealant did not show differences between themselves and in relation to the other groups (Fig. 10-E).

Discussion

In this study, the model of nerve injury chosen was the complete transection of the ischiatic nerve (neurotmese), followed by burial of the nervous stumps next to the adjacent musculature. This type of model was chosen considering that neurotmesis is the most severe form of peripheral nerve injury, with no complete

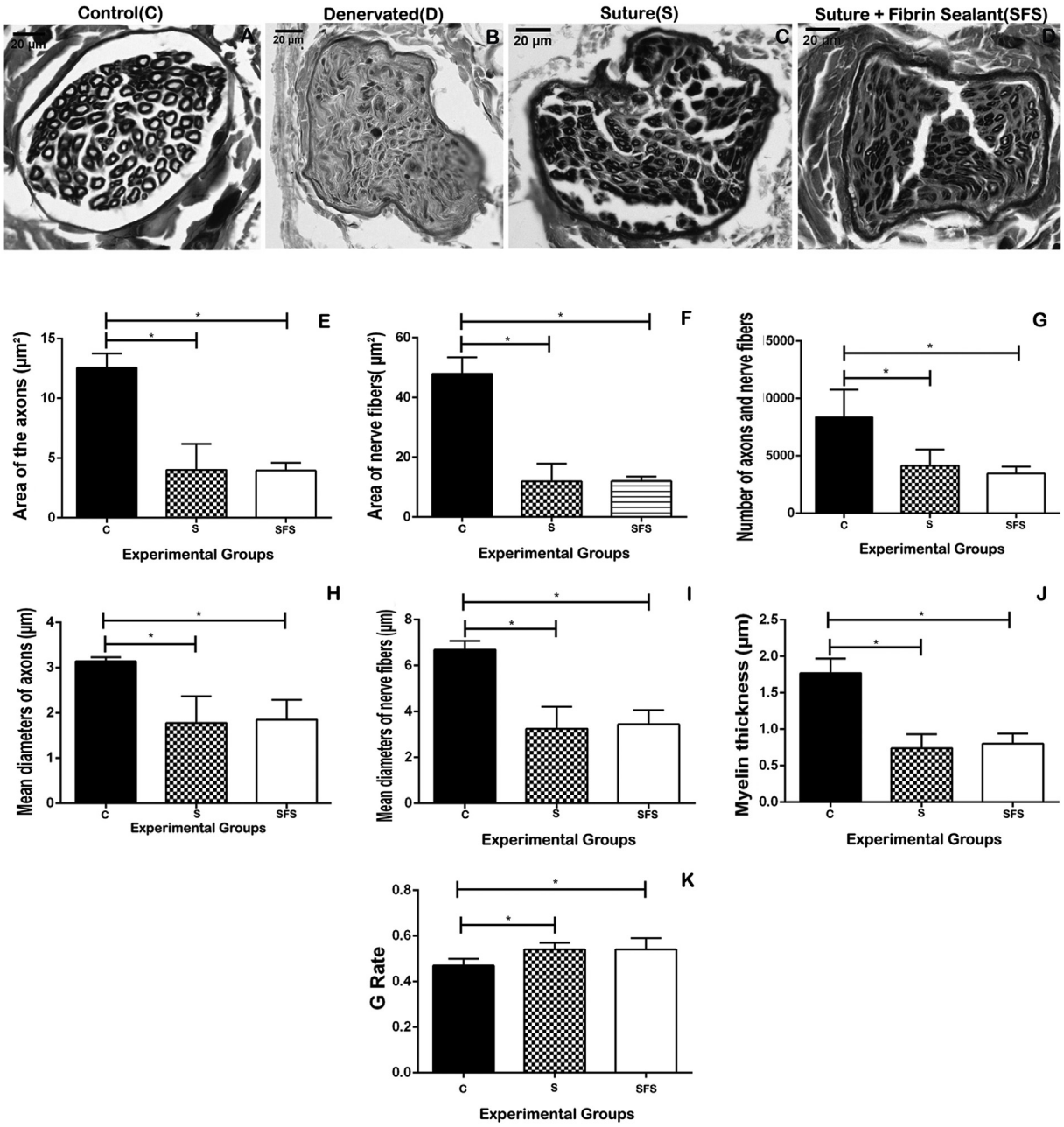

Fig. 5. A-D: Photomicrographs of transverse sections of the tibial nerve muscle branch, stained in osmium tetroxide. A: Control group (C); B: Denervated group (D); C: Suture group (S); D: Suture + Fibrin Sealant group (SFS). E-K: Graphs of the means and standard deviation of the morphometric analysis of the muscle branch of the tibial nerve for the soleus muscle of the C, S and SFS groups. E: Area of axons (µm2); F: Area of nerve fibers (µm2); G: number of axons and nerve fibers. H: axon diameter (µm); I: nerve fiber diameter (µm); J: Thickness of myelin sheath (µm); K: ratio G. E,F,H–K : Technique of analysis of variance for the model with one factor complemented by test of multiple comparisons of Tukey (Zar, 2009), *$p < 0.05$. G: Technique for analysis of non-parametric variance (Kruskal-Wallis test) for the model with factor complemented by Dunn's multiple comparison test (Zar, 2009),* $p < 0.05$).
*This analysis was not performed in group D animals, due to the absence of regenerated nerve fibers.

functional recovery [31]. The burial of stumps was performed to avoid spontaneous regeneration, considering that the peripheral nervous system has a remarkable ability to regenerate after nerve damage, even though the distance between the stumps resulting from injury restrain axonal growth, limit the regeneration process [32]. In the search for new methods, in order to achieve better morphological and functional recovery, the association of the new fibrin sealant (CEVAP) at only one point of suture, which reduces the points used in the conventional technique, has been chosen in this study as a methodology for nerve reconstruction. This sealant, developed by CEVAP, Unesp, Botucatu, SP, Brazil, has the singularity of being free of human blood, which makes the CEVAP fibrin sealant a distinct product from the existing, commercially available ones, having the important advantage of reduced adverse reactions [14].

The period of 7 days for post-injury reconstruction was chosen in order to observe the action of the sealant used, given that after this period nervous degeneration is well established [33]. In addition, although delayed nerve reconstruction is expected to impair recovery [34], this type of injury is commonly accompanied by other major trauma requiring urgent treatment; so the choice of this period can simulate this real life situation.

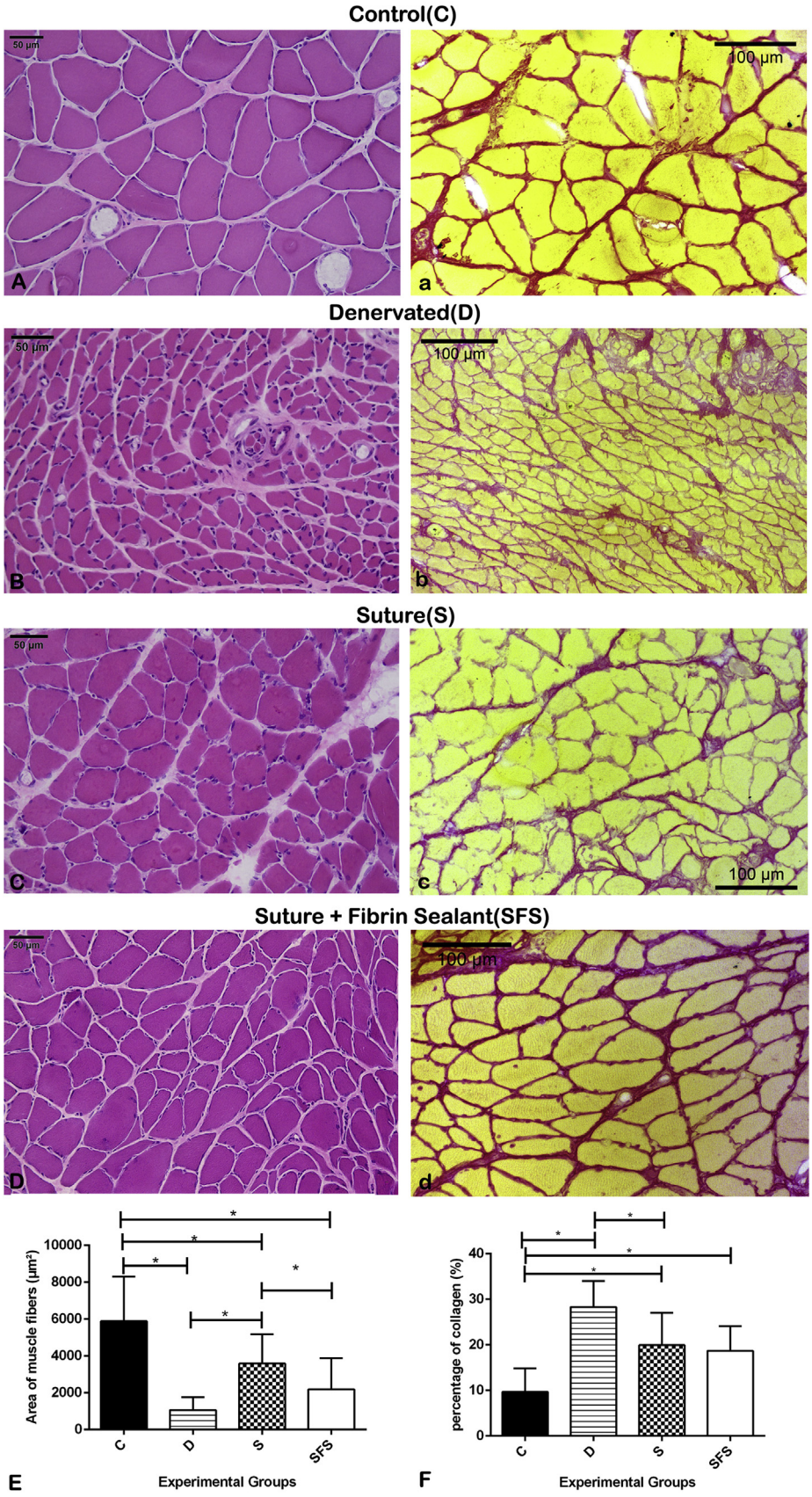

Fig. 6. Photomicrographs of cross sections of the soleus muscle stained with HE (A-D) and Picrossirius Red (a–d) from all experimental groups, under conventional light microscopy. (E) Graph of the Mean and Standard Deviation values of the area of muscle fibers for all experimental groups. ($p < 0.05$, technique for analysis of variance for the one-factor model complemented by the Tukey's multiple comparison test). (F) Graph of the percentage of collagen for all experimental groups. (Technique of analysis of variance for the model with one factor complemented by the Tukey's multiple comparison test (Zar, 2009, $^*p < 0.05$). (For interpretation of the references to colour in this figure legend, the reader is referred to the web version of this article).

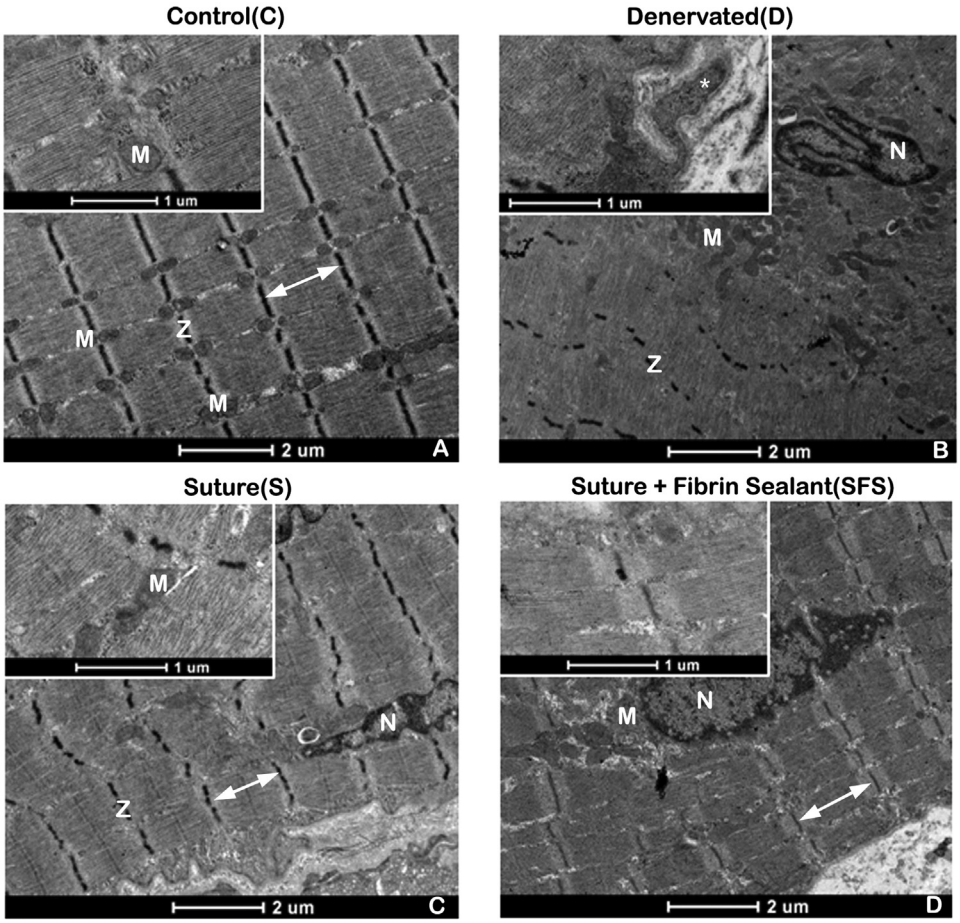

Fig. 7. Electron micrographs of muscle fibers; (M) mitochondria, (Z) Z-line, (↔) sarcomeres, (N) Nuclei.

In this study, the option to fix the stumps to the adjacent musculature after neurotmese may have provided the Denervated group with a condition for collateral reinnervation, whose functional results in relation to the ratios of the footprint area (15 and 30 days post-surgery) and contact (30 days post-surgery) obtained with the Catwalk, were higher than those of the Suture and Suture + Fibrin Sealant groups. This neurotization process is defined by the viability of muscle contraction through nerve stimuli by nerves or by other, non directly related muscles [35]. In this group it was possible to observe morphological characteristics indicative of atrophy, already well described in the literature, which result from denervation: reduction of muscle weight [36–38]and of the area of fibers [39–41], increase in the percentage of collagen [42,43], central nuclei [44]; ultraestructurally desaggregation of sarcomeres, and a discontinuous and fragmented Z line were observed [45]. Regarding neuromuscular junctions, analysis of this area was statistically smaller when compared with group Control, a finding compatible with the reduction of muscle fiber diameter [46]; ultraestructurally, empty sinaptic gutter were observed [45].

Electroneuromyography data on amplitude and latency showed that group Control had the best values, with recovery in groups Suture and Suture + Fibrin Sealant without, however reaching the values of the control group, where latency values that refer to the speed of nerve conduction were low and the Amplitude values were high, which relate to the number of muscle fibers that are able to respond to the electrical stimulus and, consequently, to the number of excitable axons.

Martins et al [47], in an experimental study comparing the exclusive use of suture and associating a suture point with fibrin glue (commercial) for nerve reconstruction, found a similar pattern for amplitude and latency in the reconstructed groups similar to the data obtained in our study. However, the latency values indicated a higher speed of conduction, compared with those obtained in our study, probably because the period studied by these authors was longer, 24 weeks (around 170 days). The period chosen in our study (60-days) was sufficient for the axons to cross the lesion site and reinerve the target organs, but for full nerve fiber maturation, a longer period might be necessary [47]. However, the amplitude values found in the Suture and Suture + Fibrin Sealant groups differed from those of Martins et al [47], being higher than those of these authors, which suggested that the same nerve impulse may have stimulated a greater number of muscle fibers.

The morphological analysis of the ischiatic nerve and the muscle branch of the tibial nerve to the soleus muscle showed this same pattern of regeneration and similarity between the Suture and Suture + Fibrin Sealant groups, whose morphology was closely related to group Control. Values for the diameter, area, number of axons and nerve fibers, and thickness of the myelin sheath of the tibial nerve were also similar in groups Suture and Suture + Fibrin Sealant. As for ischiatic nerve analysis, only the number of axons

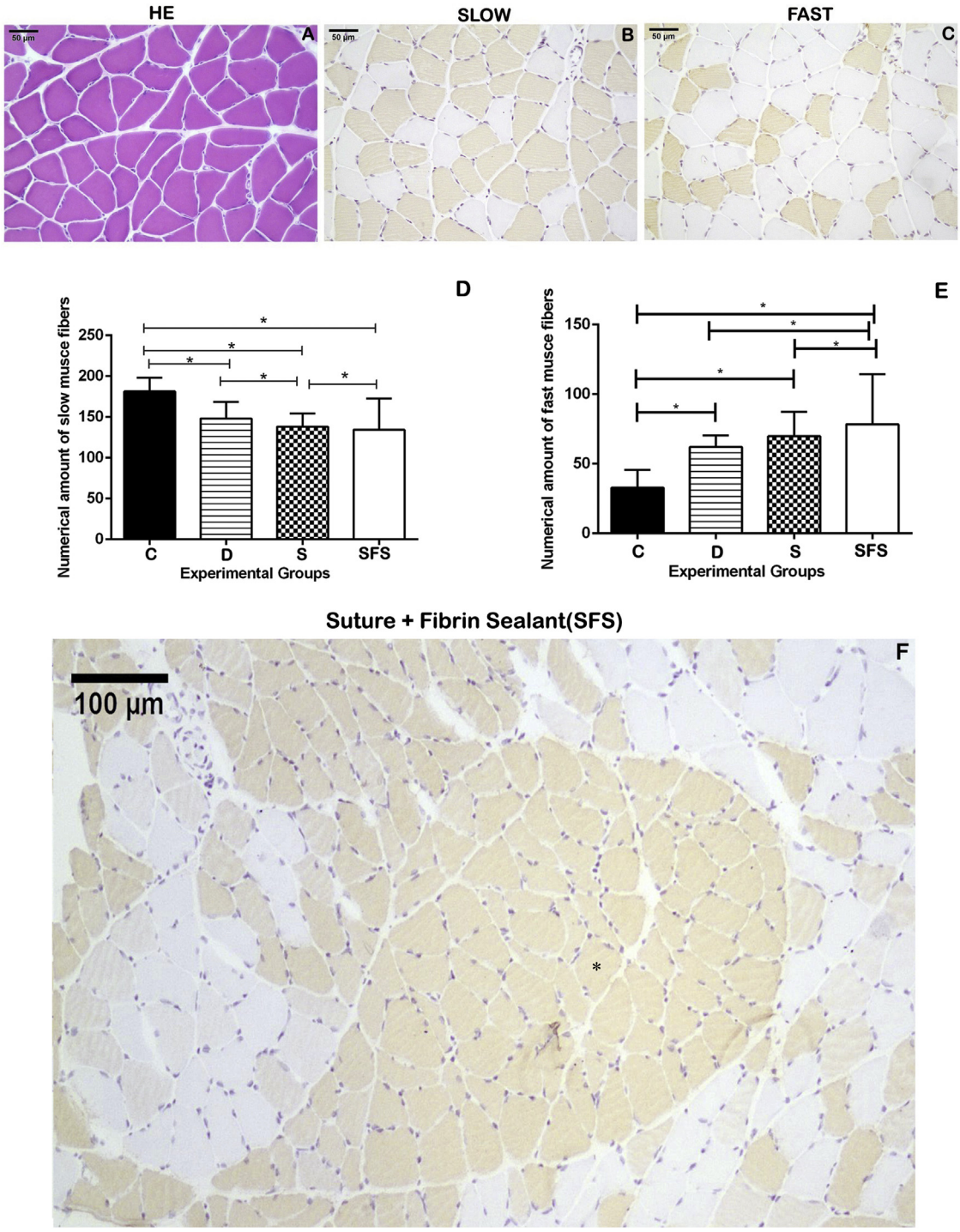

Fig. 8. A-C: Photomicrographs of transversal sections of the soleus muscle of the control group. A: HE; B: Immunohistochemistry for Slow Fiber; C: Immunohistochemistry for Fast Fiber. D and E: Graphs of the Mean and Standard Deviation values of the frequencies of Slow and Fast fiber types, respectively (technique of the non-parametric analysis of variance for the model of repeated measures in independent groups complemented by Dunn's multiple comparison test (Johnson & Wichern, 2007), $^{*}p < 0.05$). F: Cross-sectional photomicrography of the soleus muscle of the SFS group. Immunohistochemistry for Fast Fiber. Asterisk: fibers in "Type grouping".

and nerve fibers was similar between these 2 groups, while the area and diameter values were higher in the Suture + Fibrin Sealant group. Both the biological sealant and the commercial sealer used, mimic the end of the coagulation cascade, providing an environment of protection and stability in the site of reconstruction, leading to the ability to potentiate nerve regeneration [15]. The indices of myelin degeneration/regeneration were also evidenced by the G ratio found in both nerves, which were within the range of normality (between 0.4 and 0.7) for the 3 groups analyzed (C,S and SFS) [48]. These values, as well as the latency values obtained, indicate that there was remyelination of the nerve fibers. However, motor recovery results obtained by the Catwalk test showed functional deficits in all injured groups (D, S and SFS), with PFI values near -100 [25]. Lower values when compared to control animals in relation to the analyses of the paw area and the maximum contact area, both at the end of the experimental period

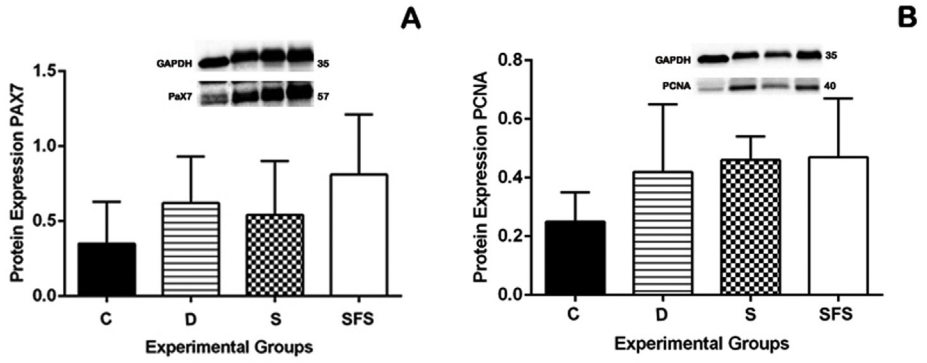

Fig. 9. Graphs of the means and standard deviation of the protein quantification of PaX7 (satellite cell marker) and PCNA (cell proliferation). Detail: protein expression of PaX7 and PCNA, respectively. (Technique of analysis of variance for the model with one factor complemented with the Tukey's multiple comparison test (Zar, 2009), *p < 0.05).

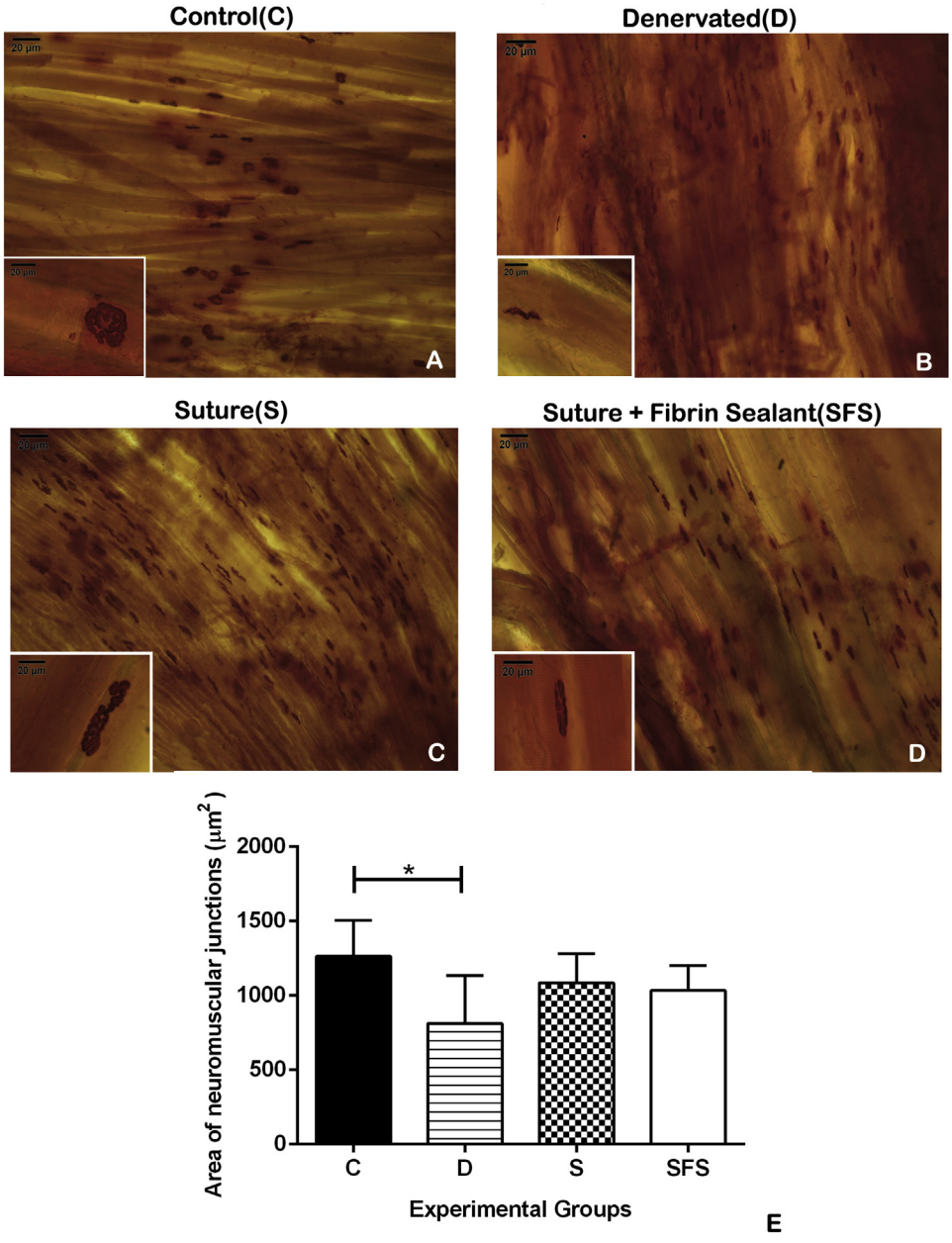

Fig. 10. A-D: Photomicrographs of the right soleus muscle (total assembly) of all experimental groups. NMJs labeled with non-specific esterase. Detail: NMJs. E: Graph of the means and standard deviation of the NMJs area (µm2) for all experimental groups. (Technique of analysis of variance for the model with a factor complemented by the Tukey's test for multiple comparisons (Zar, 2009), *p < 0.05).

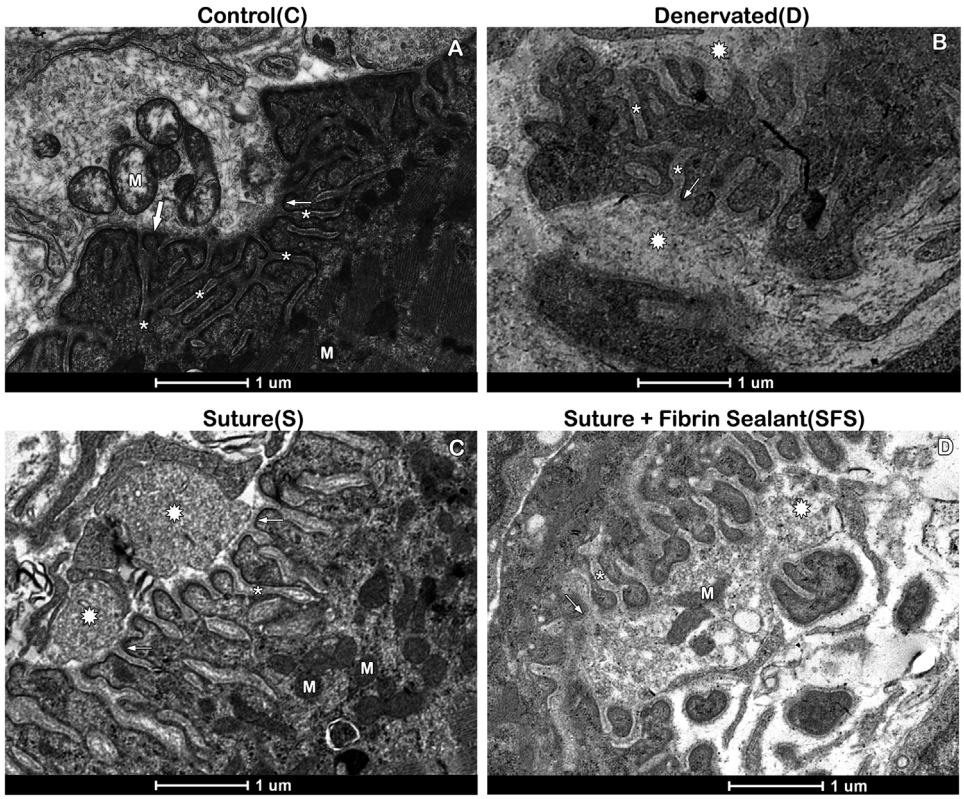

Fig. 11. Electron micrographs of NMJs. (M) mitochondria, (✡)synaptic button,(➡) active zone, (*) junction folds and (→) concentration of nAChRs.

(60 days), also indicate failure in the motor recovery. These last two parameters are directly related to the pressure exerted by the paw on the platform, and the values of these ratios close to zero indicate difficulty during support of the paw [49]. Therefore, although the previous data are indicative of axonal regeneration, the failure shown in motor recovery may be associated with the experimental period analyzed, which may not have been sufficient to promote complete nerve recovery. Cartarozzi et al [50] obtained similar results after 60 days of nerve reconstruction using stem cells + fibrin sealant as a repair technique. Studies which included longer periods of observation, such as 90 days [51] and 180 days [52] after reconstruction with suture and electrostimulation, have reported funcional improvement.

An increase of Fast fibers was detected in groups Denervated, Suture andSuture + Fibrin Sealant, with the Suture + Fibrin Sealant group showing the highest frequency of this type of fiber. According to the literature, the increase of Fast fibers is a pattern present in oxidative muscles, as has been the case of the muscle studied herein - the soleus muscle, being an indication of muscle plasticity in the case of peripheral nerve injury [53,54].

In these experimental groups, it is underscored the presence of areas containing "Type grouping", which is characterized by the presence of agglomerates of fibers of the same type. In general the normal muscle fiber is surrounded by approximately 6 muscle fibers that do not belong to its motor unit, however, in partially denervated muscles, the muscle fibers of the motor unit become progressively grouped with muscle fibers of the same type. This occurs because the muscle fibers of different motor units decrease as the muscle fibers of the same unit increase due to a reduced number of axons that regenerate and reinnervate the muscles after lesions due to nerve transection [55]. The presence of this same pattern in the denervated animals (D), reinforces the possibility of neurotization. This change in the muscular innervation pattern after peripheral nerve lesions also explains the distribution beyond the middle third of the neuromuscular junctions in the soleus muscle, where the emission of nodal roots of the last Ranvier node and of terminal and ultraterminal roots that emanated from intact muscle units close to the lesion [56], lead to competition during reinnervation, causing a polyneural innervation for a certain period of time [57].

Ultrastructurally, the presence of papillary projections on the membrane surface of the muscular fibers of the Denervated, Suture and Suture + Fibrin Sealant groups suggests of muscular atrophy [58], together with the presence of focal lesion areas still present in the Suture and Suture + Fibrin Sealant groups, are also indicative that the muscle regeneration process is not yet complete 60 days after the injury. This may also explain the fiber area results, where the values present in the Suture + Fibrin Sealant group were close to the values in group Denervated. The heterogeneity found in relation to the fiber size in the Suture + Fibrin Sealant group, by inscreasing the standard deviation, may have contributed to this similarity. In addition, in this group, fibers with large diameters, of rounded shape, have been observed, which have been found in muscular dystrophies, after trauma and as a result of atrophy after denervation [59].

The remaining morphological results showed a recovery in the animals of the Suture and Suture + Fibrin Sealant groups compared to the animals of the Denervated group, exemplified by an increase in muscle weight and a decrease in collagen percentage. This recovery in muscle mass, indicative of regeneration, was also observed after the use of acupuncture and electrical stimulation [44], of BNFD (Brain-derived neurotrophic factor) [60], and after term neurorrhaphy [61]. This improvement was also observed in the association of beta-agonist clenbuterol with end-terminal neurorrhaphy, where according to a previous study [62], an observed increase in muscle mass may be associated with reduction in protein degradation and muscle atrophy, which may also justify our study results. The data obtained in the

percentage of collagen strengthen this aspect, since the connective tissue commonly creates barriers for fusion of newly formed myotubes, which can cause failure in myogenesis [63].

Xing et al [64], correlated the increase of PaX7 to the restoration of muscle function after peripheral nerve injury and electrostimulation. PAX7 is a marker of satellite cells, which are the main cells responsible for muscle tissue regeneration, and after their activation, such cells express myogenic factors that will act in the differentiation and fusion of myotubes [65]. In the Suture + Fibrin Sealant group, the PAX7 values found suggest an increase in these cells.

In the Suture and Suture + Fibrin Sealant groups, synaptic gutter occupied by nerve terminals were observed, as reported by Sakakima et al [45], who concluded that this pattern is due to the re-encounter of the nerve terminals with the remaining post-synaptic folds. According to Sakuma et al [23], the presence of a normal ultrastructural appearance of neuromuscular junctions after prolonged denervation and reinnervation indicate that motor function failure is not due to the absence of pre or postsynaptic structural elements, but to a failure in the restoration of synaptic function.

In the treatment of the peripheral nerve injuries, use of this sealant has also been observed as easy to use, with good adhesive capacity (Buchaim et al., 2015), and further, this substance type accelerates the surgical practice [66]. The heterologous sealant has also been used in medicine, with good results in the treatment of bedsores, being easy to apply and leads to decreased pain in patients after the eighth week of use [19].

Our study results allowed us to conclude that there was a reestablishment of the nerve impulse, in addition to axonal regeneration, which was as efficient in the Suture + Fibrin Sealant group when compared with the Suture group, with superior values in the Suture + Fibrin Sealant in the lesion area (ischiatic nerve). It is an indicative of a protective effect at the lesion site due to the heterologous fibrin sealant use. It can be considered that the decrease in the number of stitches is able to reduce the trauma caused by the needle, as well as accelerating the surgical practice. So the heterologous fibrin sealant used in nerve reconstruction should be considered after peripheral nerve injury.

Conflict of interest

The authors declare they have no conflict of interest.

Acknowledgements

The authors are grateful to Carlos Roberto Padovani for the statistical expertise and consultation; processo nº 2017/06472-2, Fundação de Amparo à Pesquisa do Estado de São Paulo (FAPESP) for the funding provided; CAPES for the scholarship and Microscopy Electronic Center(CME/IBB) for the equipment used.

References

[1] Tu H, Zhang D, Corrick RM, Muelleman RL, Wadman MC, Li YL. Morphological regeneration and functional recovery of neuromuscular junctions after tourniquet-induced injuries in mouse hindlimb. Front Physiol 2017;8:207.
[2] Malomouzh AI. Non-cholinergic signaling pathways at vertebrate neuromuscular junctions. Skeletal muscle-from myogenesis to clinical relations. InTech; 2012.
[3] Tintignac LA, Brenner HR, Ruegg MA. Mechanisms regulating neuromuscular junction development and function and causes of muscle wasting. Physiol Rev 2015;95:809–52.
[4] RUVEN C, Wu W. Transplantation of embryonic spinal cord derived cells to prevent muscle atrophy after various peripheral nerve injuries. 2017 Hong Kong Inter-University Postgraduate Symposium in Biochemical Sciences. .
[5] Asplund M, Nilsson M, Jacobsson A, von Holst H. Incidence of traumatic peripheral nerve injuries and amputations in Sweden between 1998 and 2006. Neuroepidemiology 2009;(32):217–28.
[6] Sullivan R, Dailey T, Duncan K, Abel N, Borlongan CV. Peripheral nerve injury: stem cell therapy and peripheral nerve transfer. Int J Mol Sci 2016;17:.
[7] Uyanikgil Y, Cavusoglu T, Kilic KD, Yigitturk G, Celik S, Tubbs RS, et al. Useful effects of melatonin in peripheral nerve injury and development of the nervous system. J Brachial Plex Peripher Nerve Inj 2017;12:e1–6.
[8] Seddon HJ. A classification of nerve injuries. Br Med J 1942;2:237–9.
[9] Ray WZ, Mackinnon SE. Management of nerve gaps: autografts, allografts, nerve transfers, and end-to-side neurorrhaphy. Exp Neurol 2010;223:77–85.
[10] Rafijah G, Bowen AJ, Dolores C, Vitali R, Mozaffar T, Gupta R. The effects of adjuvant fibrin sealant on the surgical repair of segmental nerve defects in an animal model. J Hand Surg Am 2013;38:847–55.
[11] Wu P, Chawla A, Spinner RJ, Yu C, Yaszemski MJ, Windebank AJ, et al. Key changes in denervated muscles and their impact on regeneration and reinnervation. Neural Regen Res 2014;9:1796.
[12] Chimutengwende-Gordon M, Khan W. Recent advances and developments in neural repair and regeneration for hand surgery. Open Orthop J 2012;6:103–7.
[13] Nakamura T, Inada Y, Fukuda S, Yoshitani M, Nakada A, Itoi S, et al. Experimental study on the regeneration of peripheral nerve gaps through a polyglycolic acid-collagen (PGA-collagen) tube. Brain Res 2004;1027:18–29.
[14] Biscola NP, Cartarozzi LP, Ulian-Benitez S, Barbizan R, Castro MV, Spejo AB, et al. Multiple uses of fibrin sealant for nervous system treatment following injury and disease. J Venom Anim Toxins Incl Trop Dis 2017;23:13.
[15] Isaacs JE, McDaniel CO, Owen JR, Wayne JS. Comparative analysis of biomechanical performance of available “nerve glues”. J Hand Surg Am 2008;33:893–9.
[16] Barros LC, Ferreira Jr. RS, Barraviera SR, Stolf HO. Thomazini-Santos IA, Mendes-Giannini MJ, et al. A new fibrin sealant from Crotalus durissus terrificus venom: applications in medicine. J Toxicol Environ Health B Crit Rev 2009;12:553–71.
[17] Ferreira RS. Autologous or heterologous fibrin sealant scaffold: which is the better choice? J Venom Anim Toxins Incl Trop Dis 2014;20:31.
[18] de Oliveira Gonçalves JB, Buchaim DV, de Souza Bueno CR, Pomini KT, Barraviera B, Júnior RSF, et al. Effects of low-level laser therapy on autogenous bone graft stabilized with a new heterologous fibrin sealant. J Photochem Photobiol B Biol 2016;162:663–8.
[19] Gatti M, Vieira L, Barraviera B, SRCS Barraviera. Treatment of venous ulcers with fibrin sealant derived from snake venom. J Venom Anim Toxins Incl Trop Dis 2011;17:226–9.
[20] Perussi Biscola N, Politti Cartarozzi L, Ferreira Junior RS, Barraviera B, Leite Rodrigues de Oliveira A. Long-standing motor and sensory recovery following acute fibrin sealant based neonatal sciatic nerve repair. Neural Plast 2016;2016:.
[21] Buchaim RL, Andreo JC, Barraviera B, Ferreira Junior RS, Buchaim DV, Rosa Junior GM, et al. Effect of low-level laser therapy (LLLT) on peripheral nerve regeneration using fibrin glue derived from snake venom. Injury 2015;46:655–60.
[22] Vicente EJD, de Castro Rodrigues A, Gallacci M, Vicente PC, dos Reis Santos SM. Recuperação funcional do nervo ciático reparado pela cola de fibrina. HU Revista 2008;34:9–12.
[23] Sakuma M, Gorski G, Sheu SH, Lee S, Barrett LB, Singh B, et al. Lack of motor recovery after prolonged denervation of the neuromuscular junction is not due to regenerative failure. Eur J Neurosci 2016;43:451–62.
[24] Gasparotto VP, Landim-Alvarenga FC, Oliveira AL, Simões GF, Lima-Neto JF, Barraviera B, et al. A new fibrin sealant as a three-dimensional scaffold candidate for mesenchymal stem cells. Stem Cell Res Ther 2014;5:78.
[25] Bain J, Mackinnon S, Hunter D. Functional evaluation of complete sciatic, peroneal, and posterior tibial nerve lesions in the rat. Plast Reconstr Surg 1989;83:129–36.
[26] Sobral L, Oliveira L, Takeda S, Somazz M, Montebelo M, Teodori R. Immediate versus later exercises for rat sciatic nerve regeneration after axonotmesis: histomorphometric and functional analyses. Braz J Phys Ther 2008;12:311–6.
[27] Schneider CA, Rasband WS, Eliceiri KW. NIH Image to ImageJ: 25 years of image analysis. Nat Methods 2012;9:671–5.
[28] Lehrer GM, Ornstein L. A diazo coupling method for the electron microscopic localization of cholinesterase. J Cell Biol 1959;6:399–406.
[29] Zar J. Biostatistical analysis, 4th impression. Delhi: Dorling Kindersley (India) Pvt. Ltd; 2009 110:92.
[30] Johnson RA, Wichern DW. Applied multivariate statistical analysis. New Jersey: Prentice-Hall; 2014.
[31] Grinsell D, Keating CP. Peripheral nerve reconstruction after injury: a review of clinical and experimental therapies. Biomed Res Int 2014 698256.
[32] Gaudet AD, Popovich PG, Ramer MS. Wallerian degeneration: gaining perspective on inflammatory events after peripheral nerve injury. J Neuroinflammation 2011;8:110.
[33] Tricaud N, Park HT. Wallerian demyelination: chronicle of a cellular cataclysm. Cell Mol Life Sci 2017;1–9.
[34] Coulet B, Boretto JG, Lazerges C, Chammas M. A comparison of intercostal and partial ulnar nerve transfers in restoring elbow flexion following upper brachial plexus injury (C5-C6±C7). J Hand Surg Am 2010;35:1297–303.
[35] Giordani G, Westphal Filho RJ, et al. Tratamento da paralisia facial por neurotização. Arq Catarinenses Med 2009;38:152–4.
[36] Frost HK, Kodama A, Ekström P, Dahlin LB. G-CSF prevents caspase 3 activation in Schwann cells after sciatic nerve transection, but does not improve nerve regeneration. Neuroscience 2016;334:55–63.
[37] Higashino K, Matsuura T, Suganuma K, Yukata K, Nishisho T, Yasui N. Early changes in muscle atrophy and muscle fiber type conversion after spinal cord transection and peripheral nerve transection in rats. J Neuroeng Rehabil 2013;10:46.

[38] Michael F, Vainshtein A, Carter HN, Zhang Y, Hood DA. Denervation-induced mitochondrial dysfunction and autophagy in skeletal muscle of apoptosis-deficient animals. Am J Physiol Cell Physiol 2012;303:C447–54.
[39] Ohira T, Higashibata A, Seki M, Kurata Y, Kimura Y, Hirano H, et al. The effects of heat stress on morphological properties and intracellular signaling of denervated and intact soleus muscles in rats. Physiol Rep 2017;5: e13350.
[40] Tuffaha SH, Budihardjo JD, Sarhane KA, Khusheim M, Song D, Broyles JM, et al. Growth hormone therapy accelerates axonal regeneration, promotes motor reinnervation, and reduces muscle atrophy following peripheral nerve injury. Plast Reconstr Surg 2016;137:1771–80.
[41] Wiberg R, Jonsson S, Novikova LN, Kingham PJ. Investigation of the expression of myogenic transcription factors, microRNAs and muscle-specific E3 ubiquitin ligases in the medial gastrocnemius and soleus muscles following peripheral nerve injury. PLoS One 2015;10: e0142699.
[42] Nikolaou S, Liangjun H, Tuttle LJ, Weekley H, Christopher W, Lieber RL, et al. Contribution of denervated muscle to contractures after neonatal brachial plexus injury: not just muscle fibrosis. Muscle Nerve 2014;49:398–404.
[43] Pinheiro-Dardis CM, Russo TL. Electrical stimulation based on chronaxie increases fibrosis and modulates TWEAK/Fn14, TGF-β/myostatin, and MMP pathways in denervated muscles. Am J Phys Med Rehabil 2017;96:260–7.
[44] Su Z, Hu L, Cheng J, Klein JD, Hassounah F, Cai H, et al. Acupuncture plus low-frequency electrical stimulation (Acu-LFES) attenuates denervation-induced muscle atrophy. J Appl Physiol 2016;120:426–36.
[45] Sakakima H, Kawamata S, Kai S, Ozawa J, Matsuura N. Effects of short-term denervation and subsequent reinnervation on motor endplates and the soleus muscle in the rat. Arch Histol Cytol 2000;63:495–506.
[46] Confortim HD, Jerônimo LC, Centenaro LA, Pinheiro PFF, Brancalhão RMC, Matheus SMM, et al. Effects of aging and maternal protein restriction on the muscle fibers morphology and neuromuscular junctions of rats after nutritional recovery. Micron 2015;71:7–13.
[47] Martins RS, Siqueira MG, Silva CF, Godoy BO, Plese JP. Electrophysiologic assessment of regeneration in rat sciatic nerve repair using suture, fibrin glue or a combination of both techniques. Arq Neuropsiquiatr 2005;63:601–4.
[48] Mendonça AC, Barbieri CH, Mazzer N. Directly applied low intensity direct electric current enhances peripheral nerve regeneration in rats. J Neurosci Methods 2003;129:183–90.
[49] Gensel JC, Tovar CA, Hamers FP, Deibert RJ, Beattie MS, Bresnahan JC. Behavioral and histological characterization of unilateral cervical spinal cord contusion injury in rats. J Neurotrauma 2006;23:36–54.
[50] Cartarozzi LP, Spejo AB, Ferreira RS, Barraviera B, Duek E, Carvalho JL, et al. Mesenchymal stem cells engrafted in a fibrin scaffold stimulate Schwann cell reactivity and axonal regeneration following sciatic nerve tubulization. Brain Res Bull 2015;112:14–24.
[51] Willand MP, Chiang CD, Zhang JJ, Kemp SW, Borschel GH, Gordon T. Daily electrical muscle stimulation enhances functional recovery following nerve transection and repair in rats. Neurorehabil Neural Repair 2015;29:690–700.
[52] Maciel FO, Viterbo F, Chinaque Lde F, Souza BM. Effect of electrical stimulation of the cranial tibial muscle after end-to-side neurorrhaphy of the peroneal nerve in rats. Acta Cir Bras 2013;28:39–47.
[53] Germinario E, Esposito A, Megighian A, Midrio M, Biral D, Betto R, et al. Early changes of type 2B fibers after denervation of rat EDL skeletal muscle. J Appl Physiol 2002;92:2045–52.
[54] Patterson MF, Stephenson G, Stephenson DG. Denervation produces different single fiber phenotypes in fast-and slow-twitch hindlimb muscles of the rat. Am J Physiol Cell Physiol 2006;291:518–28.
[55] Gordon T. Nerve regeneration: understanding biology and its influence on return of function after nerve transfers. Hand Clin 2016;32:103–17.
[56] Gordon T, Hegedus J, Tam SL. Adaptive and maladaptive motor axonal sprouting in aging and motoneuron disease. Neurol Res 2004;26:174–85.
[57] Rich MM, Lichtman JW. In vivo visualization of pre- and postsynaptic changes during synapse elimination in reinnervated mouse muscle. J Neurosci 1989;9:1781–805.
[58] Engel A, Orawa E. Chapter 34: dystrophinopathies. Myology. Aggiungere: McGraw-Hill; 2004 978.
[59] Bonnemann C, Bushby K. In: Engel AG, Franzini Armstrong A, editors. The limb-girdle muscular dystrophies. Myology 3rd McGraw-Hill; 2004. p. 1077–121.
[60] Lopes CD, Gonçalves NP, Gomes CP, Saraiva MJ, Pêgo AP. BDNF gene delivery mediated by neuron-targeted nanoparticles is neuroprotective in peripheral nerve injury. Biomaterials 2017;121:83–96.
[61] Liu H-F, Chen Z-G, Lineaweaver WC, Zhang F. Can the babysitter procedure improve nerve regeneration and denervated muscle atrophy in the treatment of peripheral nerve injury? Plast Reconstr Surg 2016;138:122–31.
[62] Fitton A, Berry M, McGregor A. Preservation of denervated muscle form and function by clenbuterol in a rat model of peripheral nerve injury. J Hand Surg Am 2001;26:335–46.
[63] Borisov AB, Dedkov EI, Carlson BM. Abortive myogenesis in denervated skeletal muscle: differentiative properties of satellite cells, their migration, and block of terminal differentiation. Anat Embryol 2005;209:269–79.
[64] Xing H, Zhou M, Assinck P, Liu N. Electrical stimulation influences satellite cell differentiation after sciatic nerve crush injury in rats. Muscle Nerve 2015;51:400–11.
[65] Judson RN, Zhang RH, Rossi F. Tissue-resident mesenchymal stem/progenitor cells in skeletal muscle: collaborators or saboteurs? FEBS J 2013;280:4100–8.
[66] Felix SP, Pereira Lopes FR, Marques SA, Martinez AM. Comparison between suture and fibrin glue on repair by direct coaptation or tubulization of injured mouse sciatic nerve. Microsurgery 2013;33:468–77.